Lawrence Berkeley National Laboratory
LBL Publications

Title
Interference of Microplastics with MTT and XTT Cell Viability Assays

Permalink
https://escholarship.org/uc/item/298532jd

Journal
ACS Omega, 11(39)

ISSN
2470-1343

Authors
Osborn, L
Trinh, A
Rad, B
et al.

Publication Date
2026-10-06

DOI
10.1021/acsomega.6c07338

Copyright Information
This work is made available under the terms of a Creative Commons Attribution-NonCommercial-ShareAlike License, available at https://creativecommons.org/licenses/by-nc-sa/4.0/

Peer reviewed

eScholarship.org Powered by the California Digital Library
University of California

ACS OMEGA

Open Access

This article is licensed under CC-BY-NC-ND 4.0

http://pubs.acs.org/journal/acsodf

Article

Interference of Microplastics with MTT and XTT Cell Viability Assays

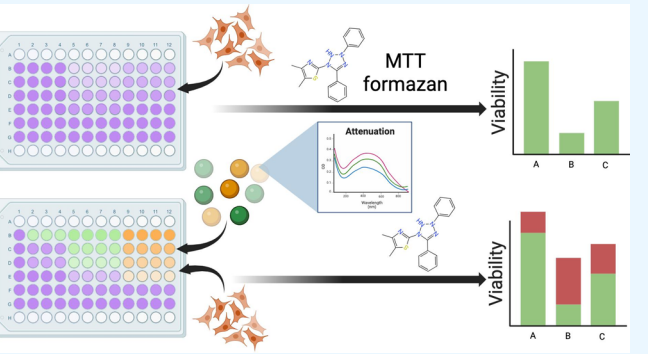
Lydia Osborn, Ajay Trinh, Behzad Rad, Aeron Tynes Hammack, and Natalia Molchanova*

Cite This: *ACS Omega* 2026, 11, 59990−60003

Read Online

ACCESS | Metrics & More | Article Recommendations | Supporting Information

ABSTRACT: Formazan-based assays like MTT and XTT are widely accepted and routinely employed colorimetric methods for assessing cell viability and metabolic activity *in vitro*. However, there is evidence that these assays are frequently subject to interference by nano- and micro-particles through various mechanisms including adsorption, abiotic reduction, and optical interference. Formazan-based assays have previously been shown to be unsuitable for applications using carbon nanotubes, metal nano- and micro-particles, and zeolite microparticles, among others. This study examines the effect of fluorescent polystyrene (PS) beads in sizes from 200 nm to 2 μm and poly(methyl methacrylate) (PMMA) beads in sizes of 1 μm and 2 μm on the accuracy of MTT and XTT cell viability assays. Our results indicate that both PS and PMMA beads cause significant interference at sizes of 1 and 2 μm due to their attenuation spectra overlapping with the measurement wavelengths of the assays. These artifacts introduce uncertainty into viability measurements as the scattering-induced attenuation of the beads masquerades as formazan absorbance, resulting in both artificially inflated and deflated metabolic activity metrics depending on particle size and assay type. The interference of smaller 200 nm particles can be effectively corrected for by washing the plate prior to analysis. We suggest that thorough washes of the plates and additional cell-free control tests are necessary before using these assays when working with microplastics.



1. INTRODUCTION

Nanoplastics (NPs) and microplastics (MPs) are recognized as an escalating global concern for both human and environmental health, stemming from the continuous degradation of larger plastic items through various mechanisms such as fragmentation, biological degradation, and chemical aging.[1] The pervasive presence of NPs and MPs in the environment leads to inevitable human exposure, primarily through ingestion of contaminated food and water, inhalation of airborne particles, and dermal contact.[2] Given these widespread exposure routes, comprehensive information regarding the toxicity of environmental NPs and MPs on human health remains largely insufficient and is an urgent concern. NPs (commonly defined as plastic particles <100 nm) and MPs (>100 nm) have previously been shown to interact with and transport across cell membranes and affect cellular processes,[3−6] with effects including induction of senescence and apoptosis, oxidative stress, and an overall decrease in cell viability.[7]

The MTT assay is by far the most common technique for measuring cell viability, maintaining popularity since its invention in 1983. The assay relies on the ability of mitochondrial succinate dehydrogenase in metabolically active cells to reduce a tetrazolium salt, MTT, into an insoluble purple formazan product.[8] In brief, after solubilizing the formazan using sodium dodecyl sulfate (SDS) or dimethyl sulfoxide (DMSO), the formazan is quantified by measuring absorbance at 570 nm on a microplate reader. The concentration of formazan produced is used as a direct proxy for the number of metabolically active cells in each well. Since its inception it has been tailored for various applications, including drug discovery, cell proliferation studies, oncology research, environmental studies, and tissue engineering.[9]

However, the long and often inconsistent solubilization step required by the MTT assay prompted the creation of alternative colorimetric assays that utilize different tetrazolium salts and produce water-soluble formazan products. One such alternative is the XTT assay, which operates under the same principles as the MTT assay but results in a water-soluble, orange formazan product and therefore needs no solubilizing agent.[10,11] The XTT assay is more rapid than the MTT assay, enabling automation and high-throughput studies, and it has become popular for measuring the viability of suspension cultures.[12−15] This assay also contains a background correction step; whereas the MTT measures absorbance only at 570 nm,

Received: June 23, 2026
Revised: September 7, 2026
Accepted: September 10, 2026
Published: September 22, 2026



Downloaded from pubs.acs.org/acsodf/article-pdf/11/39/59990/6859548/acsomega.6c07338.pdf by guest on 28 November 2026

ACS Publications

© 2026 The Authors. Published by American Chemical Society

https://doi.org/10.1021/acsomega.6c07338
ACS Omega 2026, 11, 59990−60003

Table 1. Summary of Cited Studies Concerning the Cytotoxicity of Nano- or Micro-plastics in A549 and/or BEAS-2B Cell Lines[a]

cell line(s)	type/size of NMPs	exposure time(s)	cytotoxicity assay(s)	results	ref #
A549	800 nm PS-MPs	24, 48, and 96 h	MTS assay	no reduction at 24 h. Decreased viability at 48 and 96 h. Maximum 22% reduction at 96 h at 500 μg/mL	32
A549	waste MPs (primarily PP and PE) <50 μm	24 and 48 h	MTT assay	no reduction at 24 h. 25% decrease in viability at 48 h at 100 μg/mL	3
A549, BEAS-2B	250 nm and 1 μm PS-MPs	72 h	MTT assay	20% reduction in BEAS-2B viability at 100 μg/mL of both sizes. No reduction in A549 viability	33
A549	6.2 ± 2.0 μm and 30.5 ± 10.5 μm PE-MPs	24 h	CCK-8 assay	slight reduction (~10−15%) in viability at 1000 μg/mL	34
A549	1 μm and 10 μm PS-MPs	24, 48, 72, and 96 h	MTT assay	50% decrease in metabolic activity for 1 μm at 96 h, but no reduction in viability	31
A549	80 nm PS-NPs and 2 μm PS-MPs	24 h	MTT assay	45% decrease in viability for 80 nm at 400 μg/mL. No reduction for 2 μm	35
A549	25 and 70 nm PS-NPs	24 h	MTS assay	~60% decrease in viability at 30 μg/mL of 25 nm. ~90% decrease in viability at 300 μg/mL of 70 nm. Increases in viability for both sizes up to 15 μg/mL (25 nm) and 100 μg/mL (70 nm)	36
BEAS-2B	80 nm PS-NPs	24 h	CCK-8 assay	~10% decrease in viability at 200 μg/mL	37
BEAS-2B	~100 nm PS-NPs	24 h	WST-1 assay, MTT assay	no reduction in viability up to 400 μg/mL	38
BEAS-2B	100 nm PS-NPs and 200 nm PS-MPs	24 h	CCK-8 assay	~20% decrease in viability for both sizes at 400 μg/mL	39

[a]The table does not represent a comprehensive list of studies in the field.

the XTT measures absorbance at both 450 and 660 nm. The 660 nm measurement is subtracted from the 450 nm measurement, accounting for non-specific interference such as turbidity, cell debris, or bubbles. In theory, this makes the final viability value more accurately reflect only the metabolic conversion of the reagent by active cells.

Formazan-based assays have recently been shown to be unreliable for accurately measuring the viability of cell cultures incubated with various microparticles including carbon nanotubes (CNTs),[16] porous silicon (PSi) microparticles,[17] polyethylene glycol (PEG)-coated gold nanoparticles (Au-PEG nanoparticles),[18] diesel, soot, and carbonaceous particles,[19] metal oxides and zeolite microparticles,[20,21] and superoxide-forming nanoscale TiO_2[22] due to interference of the particles with the development or measurement of various formazan products. Small molecules such as vitamin E isomers,[23] glutathione, thiols combined with carboxylic acids and amines, and acetylated amines[24] have also been shown to interact with MTT and skew results. Particulate matter exhibits distinct physicochemical properties compared to the dissolved compounds for which conventional viability assays were originally validated, introducing a range of potential artifacts and biases including chemical impurities, heteroagglomeration, nutrient depletion, fluorescent dye leaching, and direct interference with assay measurement methods.[25] Published mechanisms of interference include adsorption of formazan products,[16] abiotic reduction of formazan by microparticles,[17,19,20,22,23] and optical interference at the wavelengths of the assays.[18−21] Despite these limitations, these assays remain the most widely used methods for assessing the toxicity of CNTs, engineered particles, and many other nano- and micro-particles including microplastics.

In the existing literature, formazan-based assays (especially the MTT assay) have been broadly utilized for reporting the cytotoxicity of NMPs in a range of mammalian cell lines.[26−30] A variety of studies on A549 human adenocarcinomic alveolar basal epithelial cells and BEAS-2B human immortalized bronchial epithelial cells have tested exposure to a wide range of plastic bead types and sizes ranging from 25 nm to 50 μm. These studies have produced conflicting results on the presence and severity of cytotoxicity and its correlation with size (Table 1). Importantly, to our best knowledge, studies have not reported performing any wash steps intended to remove excess plastic particles and counteract potential interference, although Goodman et al. did report subtracting the absorbance of PS-MP beads alone to account for potential interference.[31] Considering the variability in results under similar experimental conditions as well as previously established limitations of formazan-based assays, there has been a surprising lack of investigation into how the plastic beads themselves might interact with the assays.

The XTT assay is less commonly used for MP research. However, it has been frequently used for general viability measurements in both A549[40,41] and BEAS-2B[42] cells, as well as a variety of cellular biology techniques including developing 3D culture mimicking the extracellular matrix,[43] cytotoxicity screenings to replace animal testing,[43,44] and evaluation of preclinical biomaterials.[45]

In this study, we built on the existing evidence of nano- and micro-particle optical interference with plate reader assays by evaluating the use of and potential issues with formazan-based assays in the growing field of microplastic research. We investigated the cytotoxicity of fluorescent polystyrene (PS) and poly(methyl methacrylate) (PMMA) beads of various sizes on A549 and BEAS-2B cells using both MTT and XTT assays in order to explore potential interference. Results generated with the MTT and XTT assays were compared to results of manual viability measurements with the trypan blue exclusion assay. Additionally, we examined the attenuation spectra of both fluorescent and non-fluorescent PS beads to determine the potential impact of fluorescence. Using this data, we assessed whether the MP beads exhibited a similar pattern of optical interference as previously studied microparticles.

2. RESULTS AND DISCUSSION

2.1. Fluorescent Microplastic Optical Density

We measured optical density (OD) values generated by each type of MP alone across a range of wavelengths encompassing

Downloaded from pubs.acs.org/acsodf/article-pdf/11/39/59990/6859548/acsomega.6c07338.pdf by guest on 28 November 2026

https://doi.org/10.1021/acsomega.6c07338
ACS Omega 2026, 11, 59990−60003

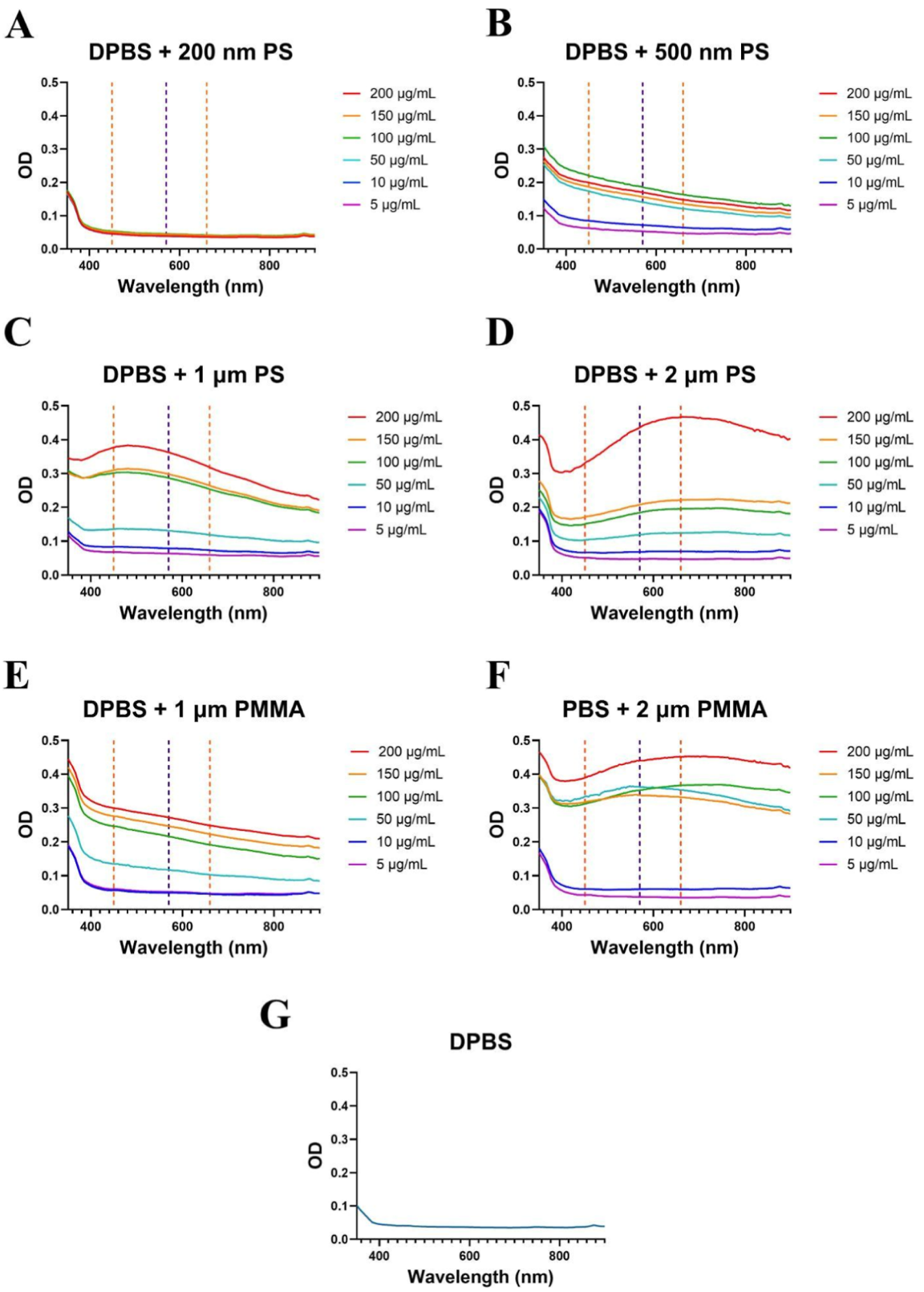


Figure 1. OD spectra of MP beads suspended in DPBS, measured from 350 to 900 nm. PS beads in sizes of (A) 200 nm, (B) 500 nm, (C) 1 μm, and (D) 2 μm. PMMA beads in sizes of (E) 1 μm and (F) 2 μm. (G) Shows the attenuation spectrum of wells containing only DPBS. Orange vertical dashed lines are at 450 and 660 nm (XTT), and purple vertical dashed lines are at 570 nm (MTT). For all, $n \geq 4$.

all the relevant assay measurements. Because these samples contained no cells or formazan that would absorb light, the results represented the light attenuation (loss) caused by the MP beads alone. Assays with MPs measured the optical attenuation at a single wavelength defined by each assay, either in the presence or absence of cells, to quantify the amount of light that reached the optical detector along the line of sight from the light source after passing through each sample. Both

Downloaded from pubs.acs.org/acsodf/article-pdf/11/39/59990/6859548/acsomega.6c07338.pdf by guest on 28 November 2026

https://doi.org/10.1021/acsomega.6c07338
ACS Omega 2026, 11, 59990−60003

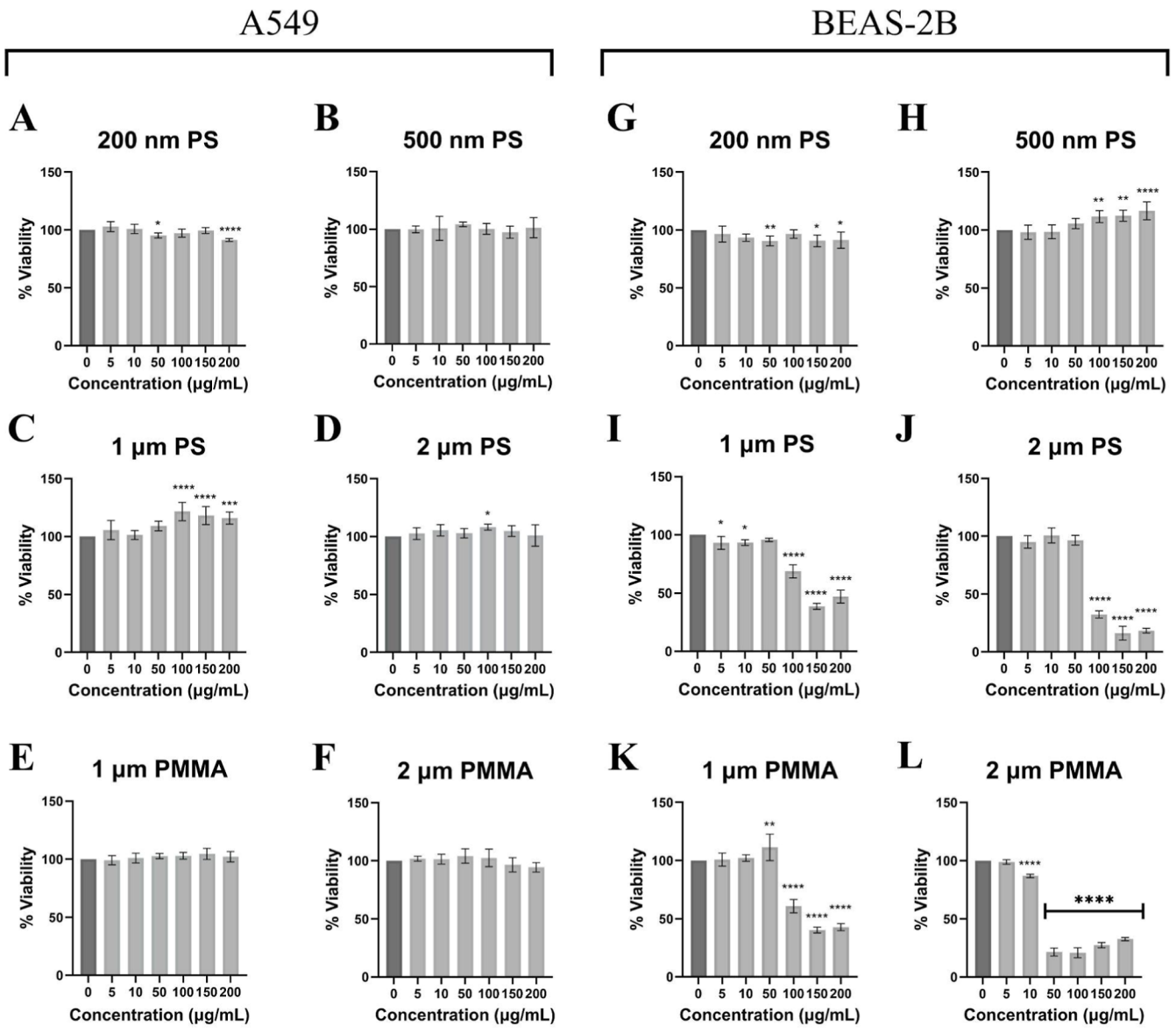


Figure 2. Cell viability of A549 (left) and BEAS-2B (right) cells measured with the MTT assay. (A–F) Show A549 cells and (G–L) show BEAS-2B cells incubated with varying concentrations and sizes of MP beads. All values are normalized to a control, which was set to 100. Data are presented as mean ± SD (*$P < 0.05$), (**$P < 0.01$), (***$P < 0.001$), (****$P < 0.0001$). All unlabeled bars are $P > 0.05$. Full heatmaps of Tukey's HSD test P values are shown in Figures S8 and S9. For all, $n \geq 6$.

assays tested rely on the absorption of light by formazan; therefore, the resulting values reflected both the light absorbed by formazan as well as the light that was scattered or absorbed by the MP beads, as measured in the MP OD spectra. When the law of conservation of energy is applied to optical radiation, the breakdown of the incoming photon energy can be represented by the following equation: $I_{\text{incident}}(\lambda) = I_{\text{transmitted}}(\lambda) + I_{\text{absorbed}}(\lambda) + I_{\text{scattered}}(\lambda) + I_{\text{reflected}}(\lambda)$.[46,47] The sum of the latter three terms on the right hand side of this equation comprise total attenuation. Considering the lack of specificity in traditional absorbance-based assay measurements, results termed "absorbance values" are, in reality, composed of both the absorbance of formazan as well as any scattering or absorption caused by the MPs. Particles on the nanometer scale generally follow Rayleigh's rule and scattering within visible and NIR/NUV wavelengths can be reasonably ignored, but the sizes of MPs tested here (200 nm to 2 μm) are in the Mie regime and therefore scattering is potentially significant.[46,47] Furthermore, in their study He et al. established that polystyrene beads exhibit near-perfect transparency between 300 and 1300 nm, with absorption only occurring in the deep UV range (<300 nm).[48] Because the particles are predominantly non-absorbing in our experimental window (350–900 nm), the particle absorption coefficient is negligible. Consequently, the particle-induced attenuation is entirely dominated by the light scattering coefficient. This pure-scattering assumption has been validated as Mie theory calculations assuming zero particle absorption show excellent agreement (within 5%) with experimental attenuation spectra across a wide range of bead sizes (20 nm to 85 μm). Additionally, because PMMA possesses a high visible light transmittance of approximately 92%, its light absorption is physically negligible.[49] Much like the polystyrene beads, this lack of absorption means that light attenuation is driven purely by scattering, making it highly suitable for analysis under general Mie theory.

Downloaded from pubs.acs.org/acsodf/article-pdf/11/39/59990/6859548/acsomega.6c07338.pdf by guest on 28 November 2026

https://doi.org/10.1021/acsomega.6c07338
ACS Omega 2026, 11, 59990–60003

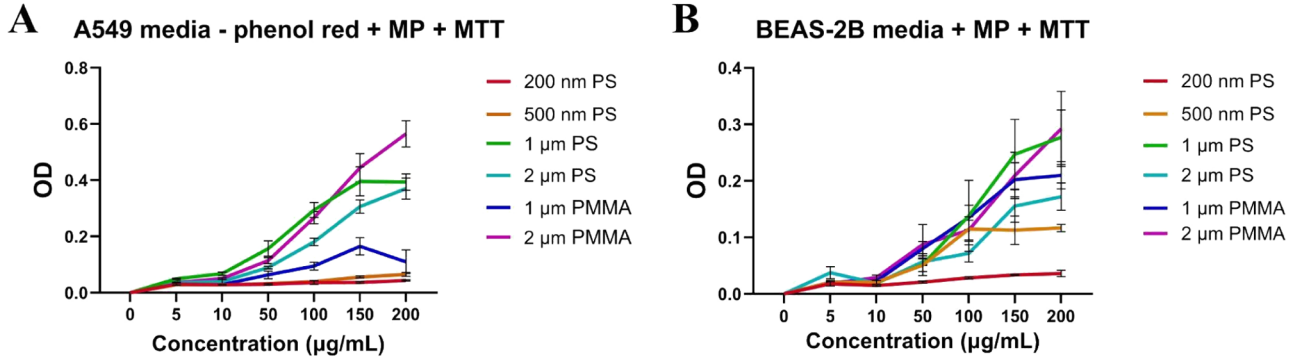


Figure 3. OD (interpreted as absorbance) measurements of MP beads alone at 570 nm after performing MTT assay in (A) A549 media without phenol red and (B) BEAS-2B media. In the MTT assay, scattering is presumed to be negligible, so OD values are normally considered equivalent to and are labeled as absorbance values. All values are normalized to a control, which was set to 0. For all, $n \geq 4$.

To establish a baseline of potential optical interference, attenuation spectra of each type, size, and concentration of MP suspended in DPBS were taken at wavelengths from 350 to 900 nm. As mentioned above, attenuation refers to the total reduction of light intensity reaching the optical detector after passing through the sample medium. Wells were incubated with MPs for 24 h and washed twice with 100 μL/well of DPBS before starting each OD measurement. Under ideal washing conditions this would suspend and remove all MP beads and result in OD spectra identical to the control spectrum of DPBS alone. However, the significant differences between the MP spectra and the control indicate that the beads are not fully removed by washing and are likely sticking to the wells.

The resulting spectra show a consistent increasing trend in OD correlating with both MP size and concentration (Figure 1A−F). The 200 nm PS beads had similar OD values to control wells with DPBS only, suggesting that its scattering-induced attenuation might be negligible when measuring plates with cells (Figure 1A). All other MP types and sizes caused varying degrees of non-negligible attenuation. The 500 nm PS, 1 μm PS, and 1 μm PMMA beads all exhibited decreasing OD trends as wavelength increased, with the 500 nm PS beads generating lower OD values than either of the 1 μm beads (Figure 1B,C,E). While the 1 μm beads produced consistently decreasing OD effects as wavelength increased, the 2 μm beads reached their maximum OD around 660 nm (Figure 1D,F). The 2 μm beads also had the highest OD values of all the sizes, and values were slightly higher for PMMA beads than for PS at both sizes. The control spectra of DPBS alone confirms that there were no peaks inherent in the background from the solvent or the plate itself (Figure 1G). Attenuation spectra were also taken for PS and PMMA beads incubated in all media conditions tested and with XTT reagent to ensure that the effects of phenol red and MTT/XTT reagent were not impacting the OD trends (Figures S1−S3). None of the media components had an effect at the wavelengths used to measure XTT, but as expected phenol red displayed a small peak at the wavelength used to measure MTT (Figure S1). Therefore, all MTT experiments were conducted in media without phenol red. For the purposes of remaining consistent with the assay protocols, measurements from assays performed with cells will be termed "viability" whereas measurements from assays performed without cells will be termed "OD" or "attenuation spectra".

2.2. Fluorescent Microplastic Interference with MTT Assay

2.2.1. Cell Viability of A549 and BEAS-2B Cells Exposed to MPs Measured with MTT. In order to reduce the potential for MP interference while minimally affecting metabolic activity, two gentle washes were performed prior to addition of the MTT reagent. The MTT assay reported that A549 cells displayed constant or increased viability for all MP types after a 24 h exposure (Figure 2A−F). Incubation with 200 and 500 nm PS beads at all concentrations resulted in cell metabolic activity around 100% (Figure 2A,B). Notably, cells exposed to 1 and 2 μm PMMA also exhibited no significant changes in viability (Figure 2E,F). In contrast, we observed apparent viabilities over 100% at concentrations of 100 μg/mL or greater of 1 and 2 μm PS. Cells exposed to 1 and 2 μm PS reached peak viabilities of 122% and 108%, respectively (Figure 2C,D). Across all MP types and concentrations, the intensity of purple color development indicative of formazan production in the treated wells remained visually comparable to control wells, with no clear signs of a decrease in cellular activity (Figure S4). Qualitative visual evaluations of color development (purple for the MTT assay, and orange for the XTT assay) were used as secondary assessments of approximate viability that were not affected by optical properties of the MP beads. Analysis was focused on areas where there were significant inconsistencies between approximate expected viability based on visual color development and quantitative measured viability by either assay.

When exposed to 200 nm PS, we observed the BEAS-2B cells exhibited a slight decrease in viability to 91% (Figure 2G). The viability of cells incubated with 500 nm PS increased to 116% at 200 μg/mL (Figure 2H). In contrast, exposures to 1 and 2 μm PS and PMMA all resulted in significantly decreased viability as MP concentration increased (Figure 2I−L). Surprisingly, we observed partial viability recovery at higher concentrations. For example, the viability of cells exposed to 2 μm PMMA increased from 21% at 50 μg/mL to 32.5% at 200 μg/mL ($P < 0.0001$) (Figure 2L). At 200 μg/mL, MTT results displayed 47% viability for 1 μm PS, 43% for 1 μm PMMA, 18% for 2 μm PS, and 32.5% for 2 μm PMMA (Figure 2I−L). In terms of visible formazan presence in the treated wells, all of the larger bead sizes resulted in a lack of color at various concentrations. For 1 μm PS, 2 μm PS, and 1 μm PMMA, partial color development was observed at 100 μg/mL and no color was observed at 150 and 200 μg/mL (Figures S5 and S6). For incubations with 2 μm PMMA, no color development

Downloaded from pubs.acs.org/acsodf/article-pdf/11/39/59990/6859548/acsomega.6c07338.pdf by guest on 28 November 2026

https://doi.org/10.1021/acsomega.6c07338
ACS Omega 2026, 11, 59990−60003

was observed at concentrations of 50 μg/mL and higher (Figures S5 and S6).

The minimal viability changes of A549 and BEAS-2B cells incubated with 200 nm PS beads were consistent with the negligible attenuation caused by the beads alone, indicating that results are likely accurate under these conditions (Figure 1A). Given that the larger bead sizes produced significant OD values at the 570 nm wavelength used to measure the MTT assay, we suspect that the increases in viability observed under these conditions might be due in part to MP scattering-induced attenuation. In the case of BEAS-2B cells, the increase in apparent viability correlated strongly with particle size and concentration across most of the MPs tested. The slightly increased viability caused by 500 nm PS beads is in keeping with the fact that its OD values were greater than those of 200 nm PS but less than those of the larger beads (Figure 1B). With the larger bead sizes, the total lack of visible color development in the plate at the higher concentrations indicated an absence of metabolically active cells under these conditions (Figure S6). Despite that, MTT results showed significant percentages of viable cells in those wells, indicating an issue with the absorbance measurements (Figure 2I–L). This discrepancy was also visible on a brightfield microscope prior to the addition of SDS. Control wells had a high density of visible healthy cells attached to the well whereas wells incubated with high concentrations of the larger bead sizes had very few viable cells (Figure S7).

2.2.2. Optical Density of MP Beads in Media with MTT Reagent. In order to isolate the effects of PS and PMMA beads on assay absorbance measurements, MTT assays were performed with only MP beads in the absence of cells (Figure 3). Identical washes were performed as for assays with cells present to ensure as many MP beads as possible were removed from the wells before measurement. OD values of MPs in A549 media were higher than in BEAS-2B media, but the trends were similar regardless of media composition (Figure 3). Overall, 200 nm PS beads displayed minimal OD values in both medias, implying that some particles are small enough to avoid significant interference (Figure 3). In all cases, control values were obtained by measuring the OD of cell media and MTT reagent alone.

MP attenuation in A549 media showed a clear increasing trend as particle concentration and size increased. The 500 nm PS beads exhibited similarly minimal values to the 200 nm PS beads, but the wells with 1 μm PS, 2 μm PS, and 2 μm PMMA beads produced substantial OD (Figure 3A). The values of 1 and 2 μm PS at 200 μg/mL were around 0.4 relative to a control normalized to 0, while 1 and 2 μm PMMA exhibited values around 0.11 and 0.55 greater than the control, respectively (Figure 3A). The OD measurements in BEAS-2B media were also significant, as all of the MPs except for 200 nm PS yielded appreciable values (Figure 3B). The 500 nm PS beads reached a peak OD value of 0.12 greater than the control (Figure 3B). At 200 μg/mL, the 1 μm PS and PMMA beads alone produced values of 0.27 and 0.21, respectively (Figure 3B). Similarly, the 2 μm PS and PMMA beads resulted in values of 0.17 and 0.29, respectively (Figure 3B).

We suspect that the scattering-induced attenuation of MP beads measured in addition to formazan might have influenced the >100% A549 apparent cell viability seen after exposure to 1 and 2 μm PS, although the small scale of the increases makes concrete conclusions difficult (Figure 2C–E). Comparing the OD values of MP beads in media alone to the apparent viability of BEAS-2B cells under the same conditions better illuminates the potential interference. When the 0.12 increase in OD caused by 500 nm PS beads alone is compared to the 116% viability of cells in the same conditions, it seems likely this inflated viability is influenced by the presence of the MP beads (Figure 2H). Similarly, the 0.29 elevated OD caused by 2 μm PMMA alone is comparable to the 32% viability measured under the same conditions (Figure 2L). The OD values of 1 μm PS and PMMA alone are potentially contributing to the 47% and 43% viability measurements produced in the same conditions with cells present (Figure 2I,K). Comparable values were also observed for MP concentrations of 100 and 150 μg/mL, signifying that MTT measurements showing viable cells at concentrations of 100 μg/mL and above are, in reality, likely caused in part by the scattering of the beads.

The observation that high concentrations (100 to 200 μg/mL) of the larger beads produced OD values 0.2 to 0.55 higher than the control emphasizes the potential of generating misleadingly high viability values when using the MTT assay with cells present. This error is especially clear under conditions where visible indicators of cell death such as a lack of color development or adhered cells are obvious. Consequently, the observed increases in A549 apparent cell viability cannot be confidently attributed to MP interference. However, a complete lack of formazan presence compared to control wells is easily visually identifiable, as seen with BEAS-2B cells (Figure S6). Hence, these conditions provide the best evidence of the effect of MP interference with viability values. Any significant measured viability by the MTT assay, as was observed for all the larger bead sizes at high concentrations, is in direct contrast with an expected viability within reasonable proximity to 0% based on formazan absence (Figures 2I–L and S6). In a broader sense, it is difficult to determine how much of a given trend is due to a real decrease in viable cells and how much is due to interference by the MP beads. The true percentage of viable cells is unclear because the exact amount of MP scattering-induced attenuation can be affected by several factors, including the density of cells adhered to each well and the number and effectiveness of washes. Therefore, subtracting MP OD values from the results of the MTT assay could also yield inaccurate results.

2.3. Fluorescent Microplastic Interference with XTT

2.3.1. Cell Viability of A549 and BEAS-2B Cells Exposed to MPs Measured with XTT. In order to expand the understanding of the optical interference of MP beads, the XTT assay was performed under the same conditions as described above. Identical experimental procedures to MTT assays were used across a 0–200 μg/mL concentration range with PS and PMMA beads. The data indicated that both the 450 and 660 nm measurements are sensitive to MP interference, leading to either under- or over-correction. Undercorrection occurred when the 660 nm measurement was insufficient to account for the attenuation caused by the MP beads, leading to inflated viability values, and over-correction occurred when the 660 nm measurement itself was inflated by the MP beads, leading to artificially low viability values.

The MP attenuation spectra in DPBS illustrates why the under- and over-correction observed is dependent on particle size (Figure 1). Comparing the intersections of the orange dashed lines, representing the two wavelengths of the XTT

Downloaded from pubs.acs.org/acsodf/article-pdf/11/39/59990/6859548/acsomega.6c07338.pdf by guest on 28 November 2026

https://doi.org/10.1021/acsomega.6c07338
ACS Omega 2026, 11, 59990−60003

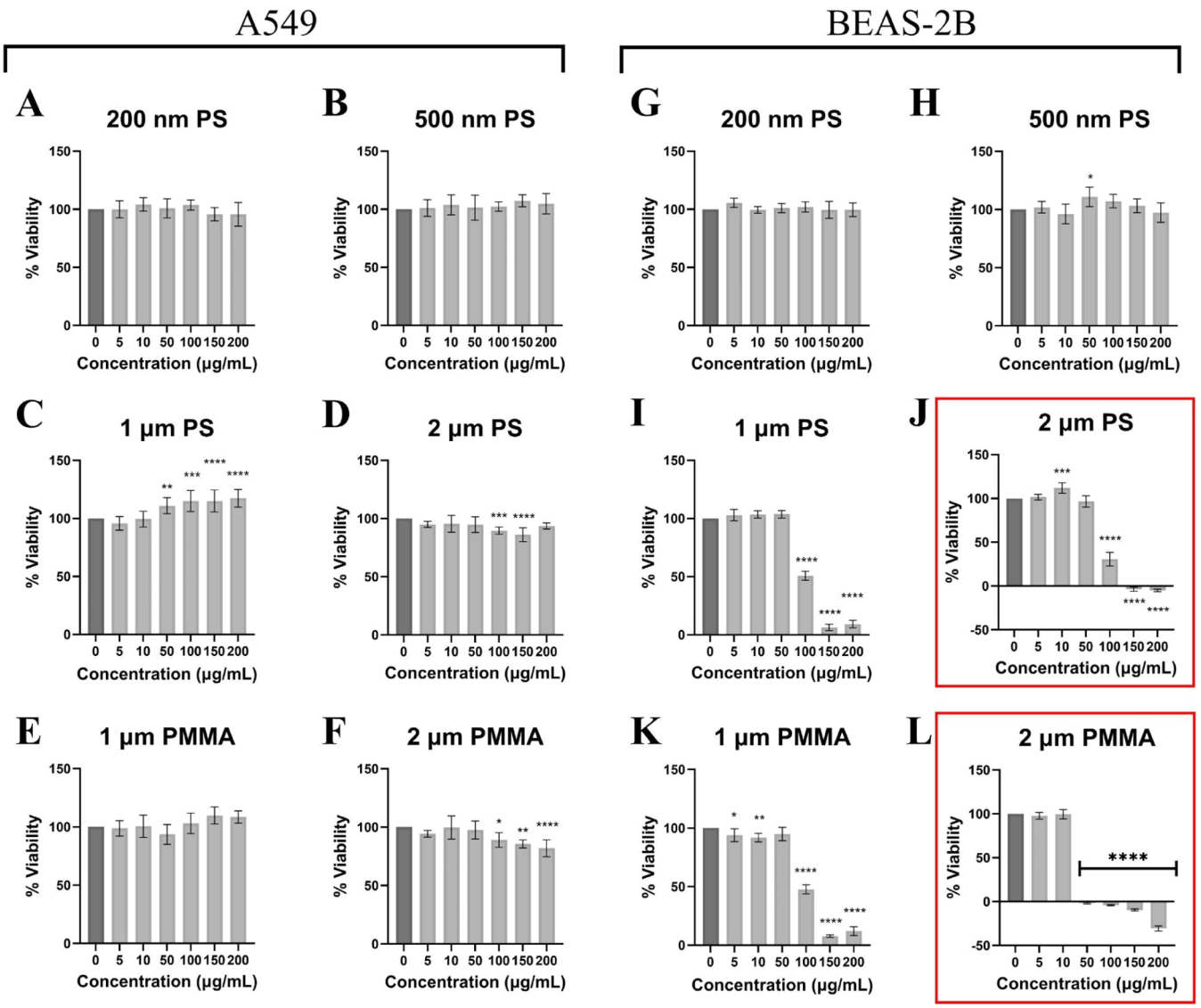


Figure 4. Cell viability of A549 (left) and BEAS-2B (right) cells measured with the XTT assay. (A−F) Show A549 cells and (G−L) show BEAS-2B cells incubated with varying concentrations and sizes of MP beads. Red boxes indicate data showing negative non-biological results. All values are normalized to a control, which was set to 100. Data are presented as mean ± SD (*$P < 0.05$), (**$P < 0.01$), (***$P < 0.001$), (****$P < 0.0001$). All unlabeled bars are $P > 0.05$. Full heatmaps of Tukey's HSD test P values are shown in Figures S12 and S13. For all, $n \geq 6$.

assay, on each graph shows how potentially effective the background correction will be at removing interference from the beads (Figure 1). The 200 nm PS showed little difference in OD between the two wavelengths (Figure 1A), indicating minimal correction effects. In contrast, 500 nm PS, 1 μm PS, and 1 μm PMMA displayed linearly decreasing OD as wavelength increased. Under these conditions, 660 nm values were lower than 450 nm values, establishing a basis for potential undercorrection (Figure 1B,C,E). The 2 μm PS and PMMA beads showed the opposite trend, where OD values at 450 nm were consistently lower than those at 660 nm (Figure 1D,F). In these cases, subtracting the 660 nm from the 450 nm measurement generated net negative OD values. These findings indicated that bead size and concentration strongly influenced wavelength-based correction in the XTT assay.

These trends were seen in both cell lines tested. A549 cells displayed consistent viability around 100% when incubated with 200 and 500 nm PS (Figure 4A,B), which is in accordance with the low MP OD values under the same conditions (Figure 1A,B). However, the 1 μm PS and PMMA beads resulted in increased viability measurements for concentrations of 100 μg/mL and above, reaching 117% and 110% at 200 μg/mL, respectively (Figure 4C,E). In contrast, incubation with 2 μm PS resulted in decreased viability measurements reaching 86% at 150 μg/mL and 93% at 200 μg/mL (Figure 4D). Incubation with 2 μm PMMA beads also resulted in decreased viability measurements reaching 85.6% at 150 μg/mL and 82% at 200 μg/mL (Figure 4F). For all concentrations and bead sizes, no change in visible orange formazan presence was observed (Figure S10).

BEAS-2B cells assessed with the XTT assay exhibited more variable viability patterns across bead sizes. Consistent with previous experiments, 200 and 500 nm PS caused only small variations around 100% viability, ranging from 96% to 105% with no directional trend (Figure 4G,H). When incubated with 1 μm PS or PMMA beads, XTT measurements indicated 6% to 9% and 8% to 12% viable cells at concentrations of 150 μg/mL and higher, respectively (Figure 4I,K). With the 2 μm beads,

Downloaded from pubs.acs.org/acsodf/article-pdf/11/39/59990/6859548/acsomega.6c07338.pdf by guest on 28 November 2026

https://doi.org/10.1021/acsomega.6c07338
ACS Omega 2026, 11, 59990−60003

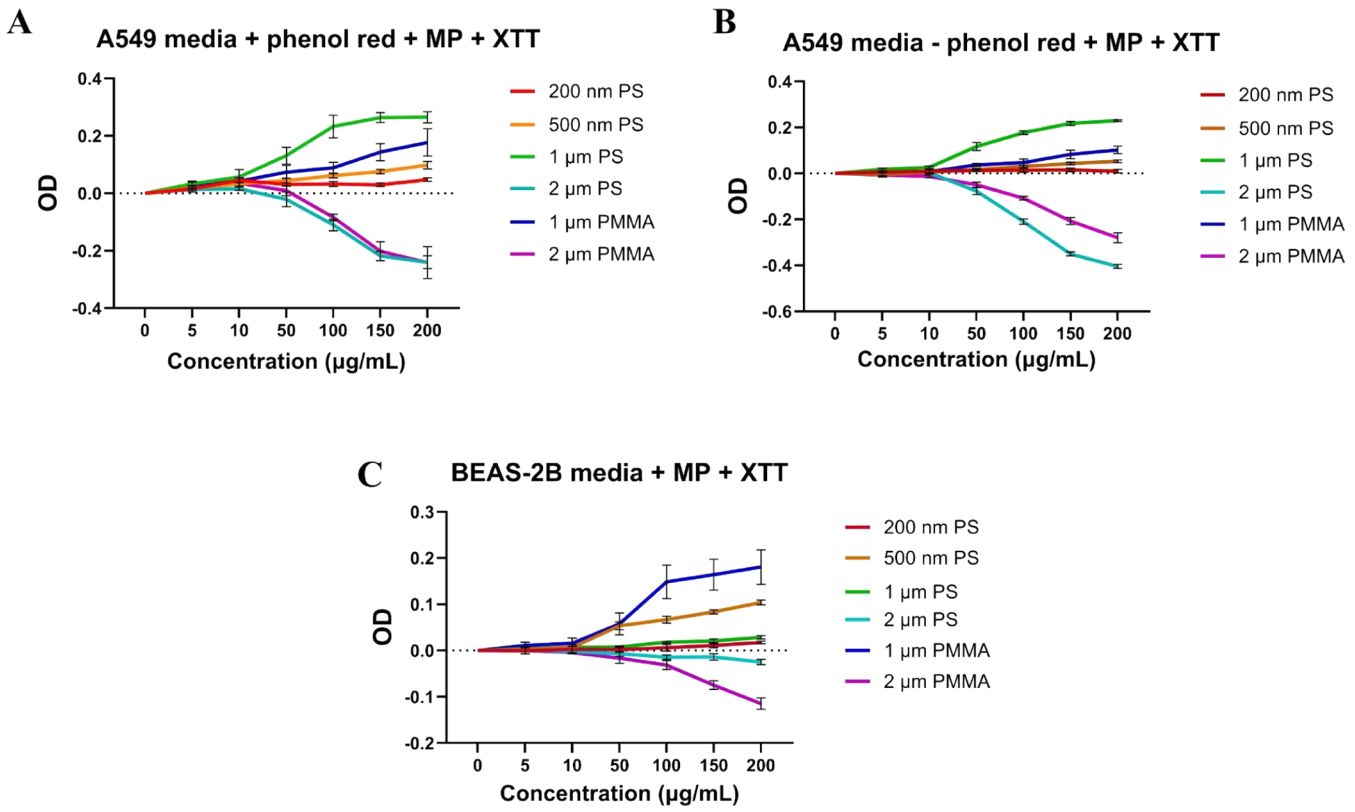


Figure 5. OD (interpreted as absorbance) measurements of MP beads alone after performing XTT assay in (A) A549 media with phenol red, (B) A549 media without phenol red, and (C) BEAS-2B media. In the XTT assay, scattering is presumed to be negligible, so OD values are normally considered equivalent to and are labeled as absorbance values. Final values were calculated by subtracting OD at 660 nm from OD at 450 nm. All values are normalized to a control, which was set to 0. For all, $n \geq 4$.

negative viabilities were recorded at the higher concentrations. Exposure to 2 μm PS caused measurements of −3.7% to −5% of metabolically active cells, and exposure to 2 μm PMMA produced −1.6% to −30.6% viability at concentrations of 50 μg/mL and higher (Figure 4J,L). There was a lack of visible orange color development in treated wells at concentrations of 150 μg/mL or higher for 1 μm PS, 1 μm PMMA, and 2 μm PS, and concentrations of 50 μg/mL or higher for 2 μm PMMA (Figure S11).

In context of the under- and over-correction patterns seen in the MP attenuation data (Figure 1), it appears possible that A549 apparent cell viability greater than 100% for the 1 μm beads and less than 100% for the 2 μm beads is due, at least in part, to the scattering-induced attenuation of the beads. Accordingly, when used to assess BEAS-2B cells, the XTT assay displayed a discrepancy between observed color development and viability values for the larger bead sizes. Significant percentages of viable cells were still measured at concentrations of 150 and 200 μg/mL of the 1 μm beads, conditions under which no color was observed (Figure 4I,K). Negative percentages of viable cells were measured at the same concentrations of the 2 μm beads, which also displayed no color development (Figure 4J,L). These pronounced inconsistencies suggest MP-induced interference in the XTT assay creates unreliable results, particularly in cells such as BEAS-2B that do exhibit variable survival rates.

2.3.2. Optical Density of MP Beads in Media with XTT Reagent. Consistent with the MTT experimental setup, the XTT assay was performed on MP beads incubated in media without any cells present to isolate MP-specific effects. There were minimal changes in OD observed with 200 nm PS beads across all media conditions, but 500 nm PS, 1 μm PS, and 1 μm PMMA beads all exhibited positive OD patterns (Figure 5). For example, in A549 media (both with and without phenol red), 1 μm PS beads generated increases in OD of 0.23 to 0.26 relative to the control, which was defined as the OD of media and XTT reagent alone. The 500 nm PS and 1 μm PMMA beads resulted in values of 0.1 and 0.17 greater than the control, respectively (Figure 5A,B). In contrast, consistently overcorrected negative OD values were observed with 2 μm MP samples. Concentrations of 200 μg/mL of 2 μm PS or PMMA alone produced decreases in OD from 0.25 to 0.4 lower than the control (Figure 5A,B). In BEAS-2B media, 1 μm PMMA caused the highest increased OD value of 0.18 (Figure 5C). The 500 nm PS beads also produced elevated values around 0.1, and 1 μm PS caused values around 0.03 (Figure 5C). Conversely, at 200 μg/mL the overcorrection of 2 μm PS and PMMA beads generated OD values 0.025 and 0.114 lower than the control, respectively (Figure 5C).

Comparing the data of MP beads alone to previous data with cells present, correlations become evident. With A549 cells present, the viabilities of cells incubated with 200 μg/mL of 1 μm PS and PMMA were around 117% and 110%, respectively (Figure 4C,E). The 0.23 and 0.17 increases in OD value produced by the same MPs alone suggest that insufficient correction by the 660 nm measurement was potentially contributing to these elevated viabilities (Figure 5B). Similarly, A549 cells exposed to high concentrations of 2 μm PS and PMMA beads displayed viability measurements around 20% lower than controls (Figure 4D,F), comparable to the OD

Downloaded from pubs.acs.org/acsodf/article-pdf/11/39/59990/6859548/acsomega.6c07338.pdf by guest on 28 November 2026

https://doi.org/10.1021/acsomega.6c07338
ACS Omega 2026, 11, 59990−60003

values around 0.25 lower than the control caused by these MPs alone (Figure 5A,B). We suggest the decrease in apparent viability was influenced by overcorrection caused by the 2 μm MP beads in tandem with potential lowered cellular metabolic activity. Accordingly, in experiments with BEAS-2B cells present, 2 μm PS beads showed slight overcorrection into negative viability values at the highest concentrations and 2 μm PMMA beads showed significant overcorrection (Figure 4J,L). The 2 μm PS beads alone produced an OD 0.025 less than the control, and with cells present the apparent viability was −5% (Figures 5C and 4J). Likewise, the experiments utilizing 2 μm PMMA beads produced significant negative values both with and without cells present, notably generating an unreasonable −30.6% viability at the highest concentration (Figures 5C and 4L). These data indicate greater under- or over-correction as MP concentration increases, artificially inflating or reducing measured viability depending on particle size. The correlation of trends between assays with MPs only and with cells present suggests that MP scattering-induced attenuation at the assay wavelengths contributes to both the negative values and the values over 100%.

2.4. Scattering-Induced Attenuation of Non-fluorescent PS Beads

To ensure that the presence of fluorophores does not play a significant role, optical attenuation spectra as well as MTT and XTT absorbance measurements were taken on 1 μm non-fluorescent PS beads. All experimental procedures were performed as previously described. The non-fluorescent PS beads displayed similar trends to their fluorescent counterpart (Figures 1C and S14B). Absorbance measurements taken after incubation with MTT or XTT reagent also exhibited comparable values to the 1 μm fluorescent PS beads in both conditions (Figures 3, 5, and S14C,D).

2.5. Independent Assessment of Cell Viability with the Trypan Blue Exclusion Assay

An independent measure of cell viability was performed to compare with values generated by the MTT and XTT assays. The trypan blue exclusion assay was chosen due to its reliance on manual cell counting and membrane permeability instead of absorbance measurements, minimizing the possibility of MP interference. Cells were incubated for 24 h with the highest concentration (200 μg/mL) of each MP type and size, after which live cells were counted under a brightfield microscope. Results indicated that A549 cells incubated with 200 μg/mL of all MP types maintained viability >90% (Figure 6A). In contrast, BEAS-2B cells exhibited significant cytotoxicity after exposure to 200 μg/mL of 1 and 2 μm PS and PMMA (Figure 6B). Under these conditions, viability ranged from 0% to 4%. Exposure to 200 and 500 nm PS had no significant effect on BEAS-2B viability. These data are consistent with the presence of formazan color development in wells incubated with 200 and 500 nm PS, and the absence of color development in wells incubated with the larger MP sizes (Figures S6 and S11).

2.6. Existing Literature on the Interference of Microparticles and Small Molecules with Formazan-Based Assays

The majority of studies on microplastics have utilized formazan-based cell viability assays, most commonly the MTT assay, to quantify viability changes. However, numerous previous studies have shown an incompatibility between formazan-based assays and various microparticles, most often due to adsorption, abiotic reduction, or optical interference.

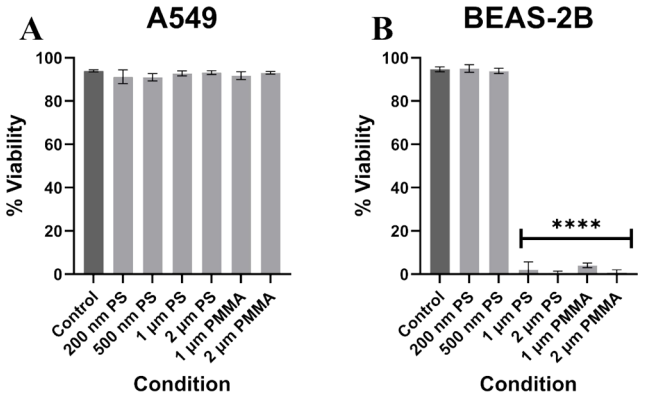


Figure 6. Cell viability of (A) A549 and (B) BEAS-2B cells incubated with 200 μg/mL of each MP type and size. Viability was measured manually with the trypan blue exclusion assay. All values are given as a percentage of live cells counted. Data are presented as mean ± SD (*P < 0.05), (**P < 0.01), (***P < 0.001), (****P < 0.0001). All unlabeled bars are P > 0.05. For all, $n \geq 3$.

Carbon nanotubes (CNTs),[16] porous silicon (PSi) microparticles,[17] polyethylene glycol (PEG)-coated gold nanoparticles,[18] diesel, soot, and carbonaceous particles,[19] metal oxides and zeolite microparticles,[20] and superoxides formed by nano-TiO_2[22] are among the list of incompatible particles. Interference via abiotic reduction by small molecules such as the vitamin E isomers α-, β-, γ-, and δ-tocotrienols and α-tocopherol,[23] as well as glutathione, thiols, and acetylated amines[24] has also been studied. Twenty years ago, Wörle-Knirsch et al. published results showing that MTT-formazan crystals attach to single-walled carbon nanotubes (SWCNTs), stabilizing the crystals and preventing solubilization, causing inaccurately low viability measurements.[50] Since then, multiple studies and literature reviews have returned similar results demonstrating various mechanisms of microparticle interference with colorimetric assays.

For example, all six common tetrazolium salts (MTT, MTS, INT, XTT, WST-1, and WST-8) have demonstrated interference with both SWCNTs and multiwalled carbon nanotubes (MWCNTs) due to strong adsorption.[16] Adsorption by the nanotubes causes the measured attenuation (interpreted as absorbance) to decrease, which is traditionally interpreted as cell death. Suni et al. showed that a standard 3 h incubation with 5 mg/mL of CNTs caused formazan levels to fall to below 70% of the control, falsely indicating that the material is cytotoxic.[16] Another study showed PSi microparticles cause spontaneous redox reactions wherein the MTT reagent is reduced to formazan while the silicon surfaces are simultaneously oxidized, a reaction that occurs regardless of the presence of cells.[17] This causes the assay to significantly overestimate cell viability. Diesel particles were also found to reduce MTT to formazan at concentrations as low as 0.05 μg/mL, creating an apparent increase in viability that masks toxic responses.[19] Similarly, cysteamine-coated quantum dots reduced MTT without any cellular metabolism, causing significant false positive results,[20,51] and the superoxide formed by incubation of nano-TiO_2 with mammalian cells reduced both MTT and XTT at different rates, rendering both assays unreliable.[22] In addition to microparticles, small molecules have also been shown to chemically interfere with formazan production. Several isomers of vitamin E that contained reducing equivalents or free thiol groups were found to

Downloaded from pubs.acs.org/acsodf/article-pdf/11/39/59990/6859548/acsomega.6c07338.pdf by guest on 28 November 2026

https://doi.org/10.1021/acsomega.6c07338
ACS Omega 2026, 11, 59990−60003

abiotically reduce MTT into formazan, producing results in A549 cells erroneously suggesting their viability increased with higher vitamin E concentrations. In the same study, the neutral red uptake (NRU) assay, which does not rely on redox reactions, provided results showing significant cytotoxicity, in agreement with microscopic observations.[23] Similarly, glutathione and thiols combined with carboxylic acids and amines abiotically reduce MTT, while acetylated amines and thiols such as mercaptosuccinic acid interfere with the MTT assay through signal suppression and overlapping absorbances.[24]

In terms of particle optical interference, Au-PEG nanoparticles absorb light at the ∼570 nm measurement window of the MTT assay, causing the raw data from cells treated with 5 nM Au-nanoparticles to falsely suggest a 22% increase in viability.[18] Similarly, soot and activated carbon also exhibited significant optical interference,[19] and various metal oxide nanoparticles absorbed light around 525 nm, which is within reasonable proximity to the absorbance of MTT-formazan to distort colorimetric measurements and yield false viability profiles.[20,21]

2.7. Comparative Analysis of MP Interference with the MTT and XTT Assays

Interference by MP beads of certain sizes is in accordance with these previous studies, especially those concerning optical interference.[18−21] Our findings demonstrate that fluorescent MP beads significantly interfere with MTT and XTT assays, joining the list of nano- and micro-particles shown to compromise these traditional methods. MP interference with the MTT assay resulted in inflated measurements of cellular metabolic activity due to minimal to significant OD values generated by MP beads in sizes of 500 nm, 1 μm, and 2 μm. At concentrations of 50 μg/mL and higher, OD values of MP beads alone in both media and DPBS were large enough to contribute to significant increases in measured viability when incubated with cells. We suggest that this interference partially masked the cytotoxicity experienced by BEAS-2B cells at high MP concentrations. While no concrete conclusions can be drawn about the effects of MP scattering and/or absorbance on MTT measurements of A549 cell viability, it is possible that MP interference played a part in the >100% viabilities observed as MP concentration increased.

We also assessed whether the 660 nm background correction measurement in the XTT assay might ameliorate the interference observed with the MTT assay. However, XTT viability measurements showed distinct correction patterns that varied from trends seen in the MTT assay. The results suggest the XTT assay is prone to both under- and over-correction dependent on concentration and strongly influenced by MP bead size. Undercorrection occurred when OD values of the MP beads at 450 nm exceeded values at 660 nm, causing the XTT-defined absorbance of the beads alone to be significantly higher than that of the control due to an insufficient correction by the 660 nm measurement. We observed that undercorrection occurred most prevalently with 1 μm beads, although 500 nm PS beads also caused undercorrection to a lesser extent. When 1 μm MP beads were incubated with BEAS-2B cells, which produced no visible formazan at concentrations at or above 150 μg/mL, undercorrection resulted in measurable percentages of viable cells in these conditions (Figures 4I−L and S10). Overcorrection occurred when MP OD values at 450 nm were lower than values at 660 nm, causing the XTT-defined absorbance of the beads to become less than the control due to subtracting the greater 660 nm value. This effect happened exclusively with 2 μm beads and was especially pronounced when no formazan was produced (evaluated qualitatively by the lack of visual orange color), in which case overcorrection artifactually shifted viability values below zero. With BEAS-2B cells present we observed that overcorrection caused negative viability, ranging from −2% to −30%, for experiments with the 2 μm beads. The slight reduction in A549 apparent cell viability to ∼80% under these conditions might be partially influenced by overcorrection, yet such minor variations preclude any firm conclusions.

Crucially, the results of the trypan blue exclusion assay are measurably different from either the MTT or XTT assay under certain conditions. Manually counting viable cells confirmed that A549 cells do not experience significant changes in viability under any MP conditions, whereas the viability of BEAS-2B cells is reduced to within error of 0% after incubation with the larger bead sizes but is unaffected by 200 and 500 nm PS beads (Figure 6). These values are in agreement with color development patterns in the plates with MTT and XTT, confirming that production of formazan in both assays show an absence of metabolically active BEAS-2B cells at the higher concentrations of MP beads (Figures S6 and S11). This consistency is in sharp contrast to the data obtained by the plate reader with the MTT and XTT assays, which displayed significant differences in measured viability under the same conditions. For example, the MTT assay measured 47% and 43% viability for BEAS-2B cells incubated with 200 μg/mL of 1 μm PS and PMMA, respectively. The exact same conditions measured with the XTT assay produced 9% and 12% viability, respectively. The trypan blue exclusion assay, also under the same conditions, measured 2.1% and 4.1% viable cells, respectively. Similar discrepancies were observed with the 2 μm beads incubated with BEAS-2B cells. The MTT assay measured 18% and 32.5% viability at 200 μg/mL of 2 μm PS and PMMA, respectively, whereas the XTT assay measured −5% and −30.6% viability under the same conditions. Conversely, the trypan blue exclusion assay generated viability values within error of 0% under both of these conditions. These observations underscore a clear inconsistency between manually assessed viability and plate reader assay results, as well as significant disagreement between the two absorbance assays.

Despite these issues of MP optical interference at sizes of 1 μm and greater, the two absorbance assays and the trypan blue assay agreed for incubations with the 200 nm PS beads, and to some extent the 500 nm PS beads as well. Both the MTT and XTT assay displayed only small changes in viability with no directional trend for A549 cells incubated with 200 or 500 nm PS (Figures 2A,B and 4A,B). BEAS-2B cells incubated with 200 nm PS were similarly consistent between the two assays (Figures 2G and 4G). MTT and XTT values under these conditions are also in agreement with the trypan blue exclusion assay, which measured viabilities between 91% and 95% for 200 and 500 nm PS incubated with both cell lines (Figure 6). These replicable findings, in addition to the low OD values generated by the MPs alone and with assay reagents, indicate that in this instance plate reader results with smaller particles can likely be trusted. Considering this, our data showed that 200 and 500 nm PS beads are not significantly toxic to either A549 or BEAS-2B cells in concentrations up to 200 μg/mL. It is important to note, then, that formazan-based assays are not

Downloaded from pubs.acs.org/acsodf/article-pdf/11/39/59990/6859548/acsomega.6c07338.pdf by guest on 28 November 2026

https://doi.org/10.1021/acsomega.6c07338
ACS Omega 2026, 11, 59990−60003

inherently unreliable for all work with nano- and micro-particles. At the concentrations tested here and after thorough washes of the plate, we see that when the particle size is small enough, scattering-induced attenuation of the particles is negligible and the assumption that OD and absorbance are equivalent is feasible, allowing for the use of standard absorbance-based assays.

However, we strongly recommend that wash steps be implemented prior to viability analysis even with particles that are small enough to avoid optical interference. After PS and PMMA beads were incubated overnight in plates, the higher concentrations (100, 150, and 200 μg/mL) of all bead sizes had formed a visible opaque layer on the bottom of the well. Two washes with media significantly decreased the density of this layer (Figure S15). Increasing the number of washes risked affecting assay results by disturbing the cells and causing cell death. Attenuation measurements taken on plates that had not been washed revealed significantly higher OD values than for the washed plates (Figure S16). After washing, the attenuation of the 200 and 500 nm PS beads had decreased to within error of the attenuation of DPBS alone, revealing that washing is highly effective for removing small particles to the degree necessary for accurate assay absorbance measurements. In contrast, the amount of attenuation caused by 1 and 2 μm MP beads even after two washes indicated that the issue of larger particle interference can be lessened but not eliminated entirely by washing. Varying concentrations of MP beads will also alter the effectiveness of washes and the amount of attenuation caused by the remaining beads. At the lower concentrations (5 and 10 μg/mL) of the 1 and 2 μm beads, the attenuation of the beads in solution was similar to that of DPBS alone, demonstrating how very low concentrations could also be used to avoid particle interference.

While the particles utilized in this study are fluorescently labeled, we determined that their fluorescent nature did not have a pronounced effect on the assay interference. The optical attenuation spectra of both fluorescent and non-fluorescent 1 μm PS beads displayed decreasing trends as wavelength increased, and OD values between the two MP types were highly similar. This consistency was also present in optical attenuation spectra taken prior to washing the plates, confirming that non-fluorescent PS beads exhibit the same pattern of scattering behavior as the fluorescent PS beads (Figures S14A and S16C). Absorbance measurements taken at the wavelengths of the MTT and XTT assays generated comparable values to the assays performed on fluorescent PS beads alone (Figures 3, 5, and S14C,D). This finding is expected as both the MTT and XTT assay are absorbance-based rather than emission-based assays.

The observed MP interference has similar characteristics to previously reported optical interference of other nano- and micro-particles. Díaz et al. demonstrated that magnetic iron/graphite, magnetite/silica, bare and poly(ethylene glycol)-(PEG)-ylated silica, and magnetite/FAU zeolite all produced significant absorbance values ranging from 0.1 to 0.8 units at 525 nm in cell-free conditions. The authors performed both the MTT assay and the trypan blue exclusion assay, which does not rely on absorbance measurement, to determine cytotoxicity. They found that the trypan blue exclusion assay consistently reported lower viability values and more significant downward trends than the MTT assay, especially for the nanoparticles that generated high absorbance values alone.[21] This inflation of viability measurements correlating with higher absorbance values in cell-free conditions is remarkably similar to the results observed here with MPs. Similarly, various carbonaceous particles were found to absorb light around 540 nm and interfere with the MTT assay. Holder et al. reported that a concentration of 3 μg/mL of flame soot particles caused a 120% increase in absorbance at 540 nm and also demonstrated a wavelength-dependent absorption spectrum, making background subtractions insufficient to fully correct for particle interference,[19] similar to our observations on the XTT assay. Ghasemi et al. evaluated the OD of Au-PEG nanoparticles and also found a wavelength-dependent spectrum with a similar shape and trend to our MP attenuation spectra. They identified peaks within the formazan measurement window that inflated viability values up to 122%, when their corrected fold change calculations indicated a 60% decrease in viability.[18] In comparison to the existing literature on the interference of nano- and micro-particles, our observations of wavelength-dependent OD spectra with peaks around the assay measurement wavelengths, elevated assay-defined absorbance values, and insufficient background corrections are consistent with the mechanism of optical interference and indicate that microplastics of certain types and sizes should be considered potentially incompatible with absorbance-based colorimetric assays.

3. CONCLUSIONS

Due to the widespread use of formazan-based assays like MTT and XTT in evaluating the environmental safety and biocompatibility of combustion and engineered particles, drug delivery systems, and commercial microplastics, inaccurate results have the potential to misrepresent *in vitro* cytotoxicity, significantly impacting the ability to evaluate new nano- and micro-materials. Given how common plate reader assays are in general for measuring a wide variety of chemical, biological, and physical processes, it is crucial to keep their limitations in mind. Therefore, when working with any type of particle of a size similar to or larger than the wavelength used in the assay(s) of choice, the assumption that scattering is negligible and total attenuation can be considered equivalent to absorbance is inherently flawed. For studying nano- and micro-plastics, we recommend that researchers implement cell-free controls to assess the possibility of particle interference (scattering-induced attenuation) and employ at least two independent, validated *in vitro* assays (such as combining a tetrazolium salt assay with a membrane integrity test or flow cytometry) to ensure the accuracy of toxicological assessment. We also recommend implementing thorough wash steps before performing any plate assay when working with particles of any size, regardless of their potential for scattering. For more reliable alternatives, it has been proposed to implement label-free techniques such as metabolomics or impedance-based sensing, which avoid the chemical and spectral interference inherent in dye-based systems.

4. MATERIALS AND METHODS

4.1. Materials

A549 (human immortalized adenocarcinoma alveolar epithelial cells) (CCL-185), BEAS-2B (human immortalized bronchial epithelial cells) (CRL-3588), airway epithelial cell basal medium (PCS-300-030), and bronchial epithelial cell growth kit (PCS-300-040) were purchased from ATCC (Manassas, VA, USA). Fluorescent polystyrene (PS) beads in sizes of 200 nm, 500 nm, 1 μm, and 2 μm (λ_{ex}/λ_{em} = 488/518 nm) and poly(methyl methacrylate) (PMMA) beads

Downloaded from pubs.acs.org/acsodf/article-pdf/11/39/59990/6859548/acsomega.6c07338.pdf by guest on 28 November 2026

https://doi.org/10.1021/acsomega.6c07338
ACS Omega 2026, 11, 59990−60003

in sizes of 1 μm and 2 μm ($\lambda_{ex}/\lambda_{em}$ = 540/580 nm) were purchased from Abvigen Inc (NJ, USA). DMEM/F-12 media, DMEM/F-12 media without phenol red, trypsin−EDTA (0.25%), DPBS, DMSO, polyvinylpyrrolidone (PVP), fetal bovine serum (FBS), penicillin−streptomycin (10,000 U/mL), trypan blue stain 0.4%, CyQUANT MTT Cell Proliferation Assay Kit, and CyQUANT XTT Cell Proliferation Assay Kit were purchased from ThermoFisher Scientific (MA, USA). Bovine collagen type I, fibronectin, bovine serum albumin (BSA), Millicell disposable hemocytometer slides, and 1 μm non-fluorescent polystyrene microbeads were purchased from Sigma-Aldrich (MO, USA).

4.2. Cell Culture

A549 cells were cultured up to passage 15 in an adherent monolayer in DMEM/F-12 media supplemented with 10% FBS and containing 100 units per milliliter penicillin and 100 μg per milliliter streptomycin in T75 flasks (VWR, USA). They were fed every 2−3 days and passaged at 80−90% confluence. Cells were cultivated at 37 °C in a humidified atmosphere with 5% CO_2.

BEAS-2B cells were cultured up to passage 15 in an adherent monolayer in airway epithelial cell basal medium (AECBM) supplemented with bronchial epithelial cell growth kit and containing 100 units per milliliter penicillin and 100 μg per milliliter streptomycin, prepared according to the manufacturer's instructions. Flasks were pre-coated with a mixture of 0.01 mg/mL fibronectin, 0.03 mg/mL bovine collagen type I, and 0.01 mg/mL BSA dissolved in complete AECBM medium. Flasks were incubated with the collagen solution at 37 °C overnight and the solution was removed before cells were seeded. Cells were detached with 0.25% trypsin −0.53 mM EDTA containing 0.5% polyvinylpyrrolidone (PVP). Cells were cultivated at 37 °C in a humidified atmosphere with 5% CO_2.

4.3. Microplastic Exposure and Absorbance-Based Viability Assays

Viability was measured using the CyQUANT MTT Cell Viability Assay Kit and the CyQUANT XTT Cell Viability Assay Kit (Invitrogen, CA, USA), following the procedures given by the manufacturer. In brief, cells were seeded at a density of 1.0×10^4 cells/well for the MTT assay and 0.5×10^4 cells/well for the XTT assay in a 96-well plate (Corning, USA) and left to adhere overnight. All MPs were sonicated and/or vortexed for 8−10 min immediately prior to the experiments according to the manufacturer's instructions. PS beads in sizes of 200 nm, 500 nm, 1 μm, and 2 μm and PMMA beads in sizes of 1 and 2 μm were added to the 96-well plate and incubated for 24 h at 37 °C. All MP types and sizes were tested in concentrations of 5, 10, 50, 100, 150, and 200 μg/mL. Plates were then washed twice with 100 μL/well of fresh, warm media before starting each assay.

For the MTT assay, 10 μL of MTT was added to treated, control, and blank wells containing 100 μL of phenol red free media. The plates were then incubated for 4 h at 37 °C, and 100 μL of SDS was added to all wells, followed by a 2 h incubation at 37 °C. After vigorous pipette mixing of all the wells, absorbance was read at 570 nm on a BioTek Synergy H1 microplate reader (Agilent, CA, USA). Data were calculated as the percentage of viable cells as compared to the control (non-treated) cells, using the following formula: $\frac{(\text{mean OD}_{\text{treated}} - \text{mean OD}_{\text{blank}})}{(\text{mean OD}_{\text{control}} - \text{mean OD}_{\text{blank}})} \times 100\%$, where "treated" indicates cells exposed to MPs, "control" indicates cells grown in media alone, and "blank" indicates cell media, MTT reagent, and SDS with no cells present according to the manufacturer's protocol.

For the XTT assay, 70 μL of fresh XTT solution was added to treated, control, and blank wells containing 100 μL of phenol red free media. Plates were incubated for 4 h at 37 °C before being read at 450 and 660 nm on a BioTek Synergy H1 microplate reader. Data were calculated as the percentage of viable cells as compared to the control (non-treated) cells, using the following formula: $\frac{((\text{mean OD}_{\text{treated 450nm}} - \text{mean OD}_{\text{blank 450nm}}) - \text{mean OD}_{\text{treated 660nm}})}{((\text{mean OD}_{\text{control 450nm}} - \text{mean OD}_{\text{blank 450nm}}) - \text{mean OD}_{\text{control 660nm}})} \times 100\%$.

4.4. Cell Viability Using the Trypan Blue Exclusion Assay

Live cell counting using trypan blue exclusion was performed according to the manufacturer's procedure. In brief, cells were seeded at a density of 1.5×10^4 cells/well in a 24-well plate (Corning, USA) and left to adhere overnight. All MPs were prepared identically as described above, and were tested at a concentration of 200 μg/mL. After a 24 h exposure, cells were harvested, mixed with an equal volume of trypan blue dye (Invitrogen, CA, USA), and added to a hemocytometer slide (Sigma-Aldrich, MO, USA). Live cells were manually counted under a brightfield microscope.

4.5. Statistical Analysis

All cell assays were performed in at least 6 replicates, and all attenuation experiments were performed in at least 4 replicates. Statistical analysis was performed using GraphPad Prism 10.0 software (GraphPad, La Jolla, CA). Data were analyzed using a one-way ANOVA followed by post-hoc multiple comparisons. To evaluate differences between treated groups and the control group, Dunnett's multiple comparisons test was employed. To evaluate all-pairwise comparisons between all treated groups, Tukey's honestly significant difference (HSD) test was used.

■ ASSOCIATED CONTENT

Supporting Information

The Supporting Information is available free of charge at https://pubs.acs.org/doi/10.1021/acsomega.6c07338.

Attenuation spectra of microplastic beads in other media conditions, heatmaps of statistical analysis results, and photographs of experimental setup (PDF)

■ AUTHOR INFORMATION

Corresponding Author

Natalia Molchanova − *Molecular Foundry Division, Lawrence Berkeley National Laboratory, Berkeley, California 94720, United States;* orcid.org/0000-0001-7643-4508; Email: nmolchanova@lbl.gov

Authors

Lydia Osborn − *Molecular Foundry Division, Lawrence Berkeley National Laboratory, Berkeley, California 94720, United States;* orcid.org/0009-0009-3806-8514

Ajay Trinh − *Molecular Foundry Division, Lawrence Berkeley National Laboratory, Berkeley, California 94720, United States*

Behzad Rad − *Molecular Foundry Division, Lawrence Berkeley National Laboratory, Berkeley, California 94720, United States;* orcid.org/0000-0001-6531-9168

Aeron Tynes Hammack − *Molecular Foundry Division, Lawrence Berkeley National Laboratory, Berkeley, California 94720, United States*

Complete contact information is available at: https://pubs.acs.org/10.1021/acsomega.6c07338

Author Contributions

The manuscript was written through contributions of all authors. All authors have given approval to the final version of the manuscript.

Notes

The authors declare no competing financial interest.

■ ACKNOWLEDGMENTS

Work at the Molecular Foundry was supported by the Office of Science, Office of Basic Energy Sciences, of the U.S.

Downloaded from pubs.acs.org/acsodf/article-pdf/11/39/59990/6859548/acsomega.6c07338.pdf by guest on 28 November 2026

https://doi.org/10.1021/acsomega.6c07338
ACS Omega 2026, 11, 59990−60003

Department of Energy under Contract No. DE-AC02-05CH11231, under user proposal number MFP-10280. The authors are grateful to colleagues at the Molecular Foundry for helpful conversations.

■ ABBREVIATIONS

PS, polystyrene; PMMA, poly(methyl methacrylate); MP, microplastic; NP, nanoplastic; OD, optical density; MTT, 3-(4,5-dimethylthiazol-2-yl)-2,5-diphenyltetrazolium bromide; XTT, 2,3-bis(2-methoxy-4-nitro-5-sulfophenyl)-2*H*-tetrazolium-5-carboxanilide; CNT, carbon nanotube; PVP, polyvinylpyrrolidone; AECBM, airway epithelial cell basal medium; FBS, fetal bovine serum; BSA, bovine serum albumin; DMSO, dimethyl sulfoxide; SDS, sodium dodecyl sulfate; DPBS, Dulbecco's phosphate-buffered saline

■ REFERENCES

(1) Kamalasekaran, K.; Sundramoorthy, A. K. A Review on Microplastics: Sources, Environmental Fate, Degradation Pathways, and Analytical Identification Methods. *RSC Adv.* **2026**, *16* (15), 13851−13874.
(2) Li, Y.; Tao, L.; Wang, Q.; Wang, F.; Li, G.; Song, M. Potential Health Impact of Microplastics: A Review of Environmental Distribution, Human Exposure, and Toxic Effects. *Environ. Health* **2023**, *1* (4), 249−257.
(3) Bengalli, R.; Zerboni, A.; Bonfanti, P.; Saibene, M.; Mehn, D.; Cella, C.; Ponti, J.; La Spina, R.; Mantecca, P. Characterization of Microparticles Derived from Waste Plastics and Their Bio-Interaction with Human Lung A549 Cells. *J. Appl. Toxicol.* **2022**, *42* (12), 2030−2044.
(4) Cortés, C.; Domenech, J.; Salazar, M.; Pastor, S.; Marcos, R.; Hernández, A. Nanoplastics as a Potential Environmental Health Factor: Effects of Polystyrene Nanoparticles on Human Intestinal Epithelial Caco-2 Cells. *Environ. Sci.: Nano* **2020**, *7* (1), 272−285.
(5) Roslan, N. S.; Lee, Y. Y.; Ibrahim, Y. S.; Tuan Anuar, S.; Yusof, K. M. K. K.; Lai, L. A.; Brentnall, T. Detection of Microplastics in Human Tissues and Organs: A Scoping Review. *J. Glob. Health* **2024**, *14*, 04179.
(6) Hwang, J.; Choi, D.; Han, S.; Jung, S. Y.; Choi, J.; Hong, J. Potential Toxicity of Polystyrene Microplastic Particles. *Sci. Rep.* **2020**, *10* (1), 7391.
(7) Sangkham, S.; Faikhaw, O.; Munkong, N.; Sakunkoo, P.; Arunlertaree, C.; Chavali, M.; Mousazadeh, M.; Tiwari, A. A Review on Microplastics and Nanoplastics in the Environment: Their Occurrence, Exposure Routes, Toxic Studies, and Potential Effects on Human Health. *Mar. Pollut. Bull.* **2022**, *181*, 113832.
(8) Mosmann, T. Rapid Colorimetric Assay for Cellular Growth and Survival: Application to Proliferation and Cytotoxicity Assays. *J. Immunol. Methods* **1983**, *65* (1), 55−63.
(9) van Meerloo, J.; Kaspers, G. J. L.; Cloos, J. Cell Sensitivity Assays: The MTT Assay. *Methods Mol. Biol.* **2011**, *731*, 237−245.
(10) Paull, K. D.; Shoemaker, R. H.; Boyd, M. R.; Parsons, J. L.; Risbood, P. A.; Barbera, W. A.; Sharma, M. N.; Baker, D. C.; Hand, E.; Scudiero, D. A.; Monks, A.; Alley, M. C.; Grote, M. The Synthesis of XTT: A New Tetrazolium Reagent That Is Bioreducible to a Water-Soluble Formazan. *J. Heterocycl. Chem.* **1988**, *25* (3), 911−914.
(11) Roehm, N. W.; Rodgers, G. H.; Hatfield, S. M.; Glasebrook, A. L. An Improved Colorimetric Assay for Cell Proliferation and Viability Utilizing the Tetrazolium Salt XTT. *J. Immunol. Methods* **1991**, *142* (2), 257−265.
(12) Kuhn, D. M.; Balkis, M.; Chandra, J.; Mukherjee, P. K.; Ghannoum, M. A. Uses and Limitations of the XTT Assay in Studies of Candida Growth and Metabolisms. *J. Clin. Microbiol.* **2003**, *41* (1), 506−508.
(13) Alfraidi, A.; Fagundes, T. C. Cell-Based Cytotoxicity Methods. *J. Apitherapy Nat.* **2018**, *1* (1), 3−12.
(14) An Absorbance-Based Assay for Cell Health and Proliferation - US. Bioprobes 78 Journal of Cell Biology Applications. https://www.thermofisher.com/us/en/home/references/newsletters-and-journals/bioprobes-journal-of-cell-biology-applications/bioprobes-78/cyquant-xtt-cell-viability-assay-absorbance-cell-health-proliferation.html (accessed May 19, 2026).
(15) Goodwin, C. J.; Holt, S. J.; Downes, S.; Marshall, N. J. Microculture Tetrazolium Assays: A Comparison between Two New Tetrazolium Salts, XTT and MTS. *J. Immunol. Methods* **1995**, *179* (1), 95−103.
(16) Suni, J.; Valkama, S.; Peltola, E. Save Your Tears for the Toxicity Assays—Carbon Nanotubes Still Fooling Scientists. *ACS Omega* **2025**, *10* (6), 5554−5562.
(17) Laaksonen, T.; Santos, H.; Vihola, H.; Salonen, J.; Riikonen, J.; Heikkilä, T.; Peltonen, L.; Kumar, N.; Murzin, D. Yu.; Lehto, V.-P.; Hirvonen, J. Failure of MTT as a Toxicity Testing Agent for Mesoporous Silicon Microparticles. *Chem. Res. Toxicol.* **2007**, *20* (12), 1913−1918.
(18) Ghasemi, M.; Turnbull, T.; Sebastian, S.; Kempson, I. The MTT Assay: Utility, Limitations, Pitfalls, and Interpretation in Bulk and Single-Cell Analysis. *Int. J. Mol. Sci.* **2021**, *22* (23), 12827.
(19) Holder, A. L.; Goth-Goldstein, R.; Lucas, D.; Koshland, C. P. Particle-Induced Artifacts in the MTT and LDH Viability Assays. *Chem. Res. Toxicol.* **2012**, *25* (9), 1885−1892.
(20) Awashra, M.; Młynarz, P. The Toxicity of Nanoparticles and Their Interaction with Cells: An in Vitro Metabolomic Perspective. *Nanoscale Adv.* **2023**, *5* (10), 2674−2723.
(21) Díaz, B.; Sánchez-Espinel, C.; Arruebo, M.; Faro, J.; de Miguel, E.; Magadán, S.; Yagüe, C.; Fernández-Pacheco, R.; Ibarra, M. R.; Santamaría, J.; González-Fernández, A. Assessing Methods for Blood Cell Cytotoxic Responses to Inorganic Nanoparticles and Nanoparticle Aggregates. *Small* **2008**, *4* (11), 2025−2034.
(22) Wang, S.; Yu, H.; Wickliffe, J. K. Limitation of the MTT and XTT Assays for Measuring Cell Viability Due to Superoxide Formation Induced by Nano-Scale TiO2. *Toxicol. In Vitro* **2011**, *25* (8), 2147−2151.
(23) Lim, S.-W.; Loh, H.-S.; Ting, K.-N.; Bradshaw, T. D.; Allaudin, Z. N. Reduction of MTT to Purple Formazan by Vitamin E Isomers in the Absence of Cells. *Trop. Life Sci. Res.* **2015**, *26* (1), 111−120.
(24) Neufeld, B. H.; Tapia, J. B.; Lutzke, A.; Reynolds, M. M. Small Molecule Interferences in Resazurin and MTT-Based Metabolic Assays in the Absence of Cells. *Anal. Chem.* **2018**, *90* (11), 6867−6876.
(25) Petersen, E. J.; Barrios, A. C.; Henry, T. B.; Johnson, M. E.; Koelmans, A. A.; Montoro Bustos, A. R.; Matheson, J.; Roesslein, M.; Zhao, J.; Xing, B. Potential Artifacts and Control Experiments in Toxicity Tests of Nanoplastic and Microplastic Particles. *Environ. Sci. Technol.* **2022**, *56* (22), 15192−15206.
(26) Stockert, J. C.; Horobin, R. W.; Colombo, L. L.; Blázquez-Castro, A. Tetrazolium Salts and Formazan Products in Cell Biology: Viability Assessment, Fluorescence Imaging, and Labeling Perspectives. *Acta Histochem.* **2018**, *120* (3), 159−167.
(27) Berridge, M. V.; Herst, P. M.; Tan, A. S. Tetrazolium Dyes as Tools in Cell Biology: New Insights into Their Cellular Reduction. *Biotechnol. Annu. Rev.* **2005**, *11*, 127−152.
(28) Merlin, J.-L.; Azzi, S.; Lignon, D.; Ramacci, C.; Zeghari, N.; Guillemin, F. MTT Assays Allow Quick and Reliable Measurement of the Response of Human Tumour Cells to Photodynamic Therapy. *Eur. J. Cancer* **1992**, *28* (8), 1452−1458.
(29) Carmichael, J.; DeGraff, W. G.; Gazdar, A. F.; Minna, J. D.; Mitchell, J. B. Evaluation of a Tetrazolium-Based Semiautomated Colorimetric Assay: Assessment of Chemosensitivity Testing. *Cancer Res.* **1987**, *47* (4), 936−942.
(30) Marshall, N. J.; Goodwin, C. J.; Holt, S. J. A Critical Assessment of the Use of Microculture Tetrazolium Assays to Measure Cell Growth and Function. *Growth Regul.* **1995**, *5* (2), 69−84.
(31) Goodman, K. E.; Hare, J. T.; Khamis, Z. I.; Hua, T.; Sang, Q.-X. A. Exposure of Human Lung Cells to Polystyrene Microplastics

Downloaded from pubs.acs.org/acsodf/article-pdf/11/39/59990/6859548/acsomega.6c07338.pdf by guest on 28 November 2026

https://doi.org/10.1021/acsomega.6c07338
ACS Omega 2026, 11, 59990−60003

Significantly Retards Cell Proliferation and Triggers Morphological Changes. *Chem. Res. Toxicol.* **2021**, *34* (4), 1069−1081.
(32) Milillo, C.; Aruffo, E.; Di Carlo, P.; Patruno, A.; Gatta, M.; Bruno, A.; Dovizio, M.; Marinelli, L.; Dimmito, M. P.; Di Giacomo, V.; Paolini, C.; Pesce, M.; Ballerini, P. Polystyrene Nanoplastics Mediate Oxidative Stress, Senescence, and Apoptosis in a Human Alveolar Epithelial Cell Line. *Front. Public Health* **2024**, *12*, 1385387.
(33) Ernhofer, B.; Spittler, A.; Ferk, F.; Mišík, M.; Zylka, M. M.; Glatt, L.; Boettiger, K.; Solta, A.; Kirchhofer, D.; Timelthaler, G.; Megyesfalvi, Z.; Kopatz, V.; Kovar, H.; Knasmueller, S.; Aigner, C.; Kenner, L.; Döme, B.; Schelch, K. Small Particles, Big Problems: Polystyrene Nanoparticles Induce DNA Damage, Oxidative Stress, Migration, and Mitogenic Pathways Predominantly in Non-Malignant Lung Cells. *J. Hazard. Mater.* **2025**, *495*, 139129.
(34) Gautam, R.; Jo, J.; Acharya, M.; Maharjan, A.; Lee, D.; Kim, C.; Kim, C.; Kim, K.; Kim, H.; Heo, Y. Evaluation of Potential Toxicity of Polyethylene Microplastics on Human Derived Cell Lines. *Sci. Total Environ.* **2022**, *838*, 156089.
(35) Shi, X.; Wang, X.; Huang, R.; Tang, C.; Hu, C.; Ning, P.; Wang, F. Cytotoxicity and Genotoxicity of Polystyrene Micro- and Nanoplastics with Different Size and Surface Modification in A549 Cells. *Int. J. Nanomed.* **2022**, *17*, 4509−4523.
(36) Xu, M.; Halimu, G.; Zhang, Q.; Song, Y.; Fu, X.; Li, Y.; Li, Y.; Zhang, H. Internalization and Toxicity: A Preliminary Study of Effects of Nanoplastic Particles on Human Lung Epithelial Cell. *Sci. Total Environ.* **2019**, *694*, 133794.
(37) Bu, W.; Jin, Y.; Zhou, Y.; Wang, F.; Zheng, D.; Liu, R.; Wang, X.; Yu, M.; Bao, S.; Zhao, R.; Li, J.; Zhou, X.; Feng, J.; Zhao, X.; Cheng, D. Polystyrene Nanoplastics-Induced Lung Epithelial Cells Ferroptosis Promotes Pulmonary Fibrosis via YY1/FTL Axis. *Mater. Today Bio* **2026**, *36*, 102738.
(38) Jeon, M. S.; Kim, J. W.; Han, Y. B.; Jeong, M. H.; Kim, H. R.; Sik Kim, H.; Park, Y. J.; Chung, K. H. Polystyrene Microplastic Particles Induce Autophagic Cell Death in BEAS-2B Human Bronchial Epithelial Cells. *Environ. Toxicol.* **2023**, *38* (2), 359−367.
(39) Wu, Y.; Wang, J.; Zhao, T.; Sun, M.; Xu, M.; Che, S.; Pan, Z.; Wu, C.; Shen, L. Polystyrene Nanoplastics Lead to Ferroptosis in the Lungs. *J. Adv. Res.* **2024**, *56*, 31−41.
(40) Günaydın, S.̧.; Sulukoğlu, E. K.; Kalın, S.̧. N.; Altay, A.; Budak, H. Diffractaic Acid Exhibits Thioredoxin Reductase 1 Inhibition in Lung Cancer A549 Cells. *J. Appl. Toxicol.* **2023**, *43* (11), 1676−1685.
(41) Ybarra, N.; Seuntjens, J. Radio-Selective Effects of a Natural Occurring Muscle-Derived Dipeptide in A549 and Normal Cell Lines. *Sci. Rep.* **2019**, *9* (1), 11513.
(42) Thaiparambil, J.; Amara, C. S.; Sen, S.; Putluri, N.; El-Zein, R. Cigarette Smoke Condensate Induces Centrosome Clustering in Normal Lung Epithelial Cells. *Cancer Med.* **2023**, *12* (7), 8499−8509.
(43) Huyck, L.; Ampe, C.; Van Troys, M. The XTT Cell Proliferation Assay Applied to Cell Layers Embedded in Three-Dimensional Matrix. *Assay Drug Dev. Technol.* **2012**, *10* (4), 382−392.
(44) Brosin, A.; Wolf, V.; Mattheus, A.; Heise, H. Use of XTT-Assay to Assess the Cytotoxicity of Different Surfactants and Metal Salts in Human Keratinocytes (HaCaT). A Feasible Method for in Vitro Testing of Skin Irritants. *Acta Derm.-Venereol.* **1997**, *77* (1), 26−28.
(45) Wang, M. O.; Etheridge, J. M.; Thompson, J. A.; Vorwald, C. E.; Dean, D.; Fisher, J. P. Evaluation of the In Vitro Cytotoxicity of Crosslinked Biomaterials. *Biomacromolecules* **2013**, *14* (5), 1321−1329.
(46) Bohren, C. F.; Huffman, D. R. *Absorption and Scattering of Light by Small Particles*, Revised reprint.; John Wiley & Sons, Ltd, 2008.
(47) Mishchenko, M. I.; Travis, L. D.; Lacis, A. A. *Scattering, Absorption, and Emission of Light by Small Particles*, Illustrated.; Cambridge University Press, 2002.
(48) He, G. S.; Qin, H.-Y.; Zheng, Q. Rayleigh, Mie, and Tyndall Scatterings of Polystyrene Microspheres in Water: Wavelength, Size, and Angle Dependences. *J. Appl. Phys.* **2009**, *105* (2), 023110.
(49) Nassier, L. F.; Shinen, M. H. Study of the Optical Properties of Poly (Methyl Methacrylate) (PMMA) by Using Spin Coating Method. *Mater. Today: Proc.* **2022**, *60*, 1660−1664.
(50) Wörle-Knirsch, J. M.; Pulskamp, K.; Krug, H. F. Oops They Did It Again! Carbon Nanotubes Hoax Scientists in Viability Assays. *Nano Lett.* **2006**, *6* (6), 1261−1268.
(51) Hoshino, A.; Fujioka, K.; Oku, T.; Suga, M.; Sasaki, Y. F.; Ohta, T.; Yasuhara, M.; Suzuki, K.; Yamamoto, K. Physicochemical Properties and Cellular Toxicity of Nanocrystal Quantum Dots Depend on Their Surface Modification. *Nano Lett.* **2004**, *4* (11), 2163−2169.

Downloaded from pubs.acs.org/acsodf/article-pdf/11/39/59990/6859548/acsomega.6c07338.pdf by guest on 28 November 2026

https://doi.org/10.1021/acsomega.6c07338
ACS Omega 2026, 11, 59990−60003